

Article

Enhanced Operation of Ice Storage System for Peak Load Management in Shopping Malls across Diverse Climate Zones

Fanghan Su ¹, Zhiyuan Wang ¹, Yue Yuan ¹, Chengcheng Song ¹, Kejun Zeng ¹, Yixing Chen ^{1,2,*}  and Rongpeng Zhang ^{2,3,*} 

¹ College of Civil Engineering, Hunan University, Changsha 410082, China; sufanghan@hnu.edu.cn (F.S.); wzhiyuan@hnu.edu.cn (Z.W.); yueyuan@hnu.edu.cn (Y.Y.); scc1996@hnu.edu.cn (C.S.); zkj13627486641@hnu.edu.cn (K.Z.)

² Key Laboratory of Building Safety and Energy Efficiency of Ministry of Education, Hunan University, Changsha 410082, China

³ School of Architecture and Planning, Hunan University, Changsha 410082, China

* Correspondence: yixingchen@hnu.edu.cn (Y.C.); zhangrongpeng@hnu.edu.cn (R.Z.)

Abstract: There exists a notable research gap concerning the application of ice storage systems in shopping mall settings at the urban scale. The characteristics of large pedestrian flow, high energy consumption, and high peak loads in shopping malls make their advantages in energy conservation. This study researches sustainable cooling solutions by undertaking an economic analysis of the ice storage systems within shopping malls across 11 distinct cities, each system operating under varied electricity pricing frameworks. The methodology begins with creating baseline mall models using AutoBPS and refining them with OpenStudio. Before starting to adjust the model, measured data were used to verify the accuracy of the baseline model, the coefficient of variation of the root mean square error (CVRMSE) and normalized mean bias error (NMBE) metrics were calculated for the model energy consumption, with CVRMSE values of 8.6% and NMBE values of 1.57% for the electricity consumption, while the metrics for the gas consumption were 12.9% and 1.24%, respectively. The study extends its inquiry to encompass comprehensive economic evaluations based on the unique electricity pricing of each city. This rigorous assessment discerns the relationship between capacity, operational strategies, and economic performance. Particularly striking are the so-called peak-shaving and valley-filling effects verified in regions characterized by lower latitudes and substantial cooling loads. The interaction between ice storage capacity and operational schedules significantly influences both economic viability and cooling efficiency. Based on the temporal dynamics of time-of-use (TOU) power pricing, a finely calibrated operational schedule for the ice storage system is proposed. This operational strategy entails charging during periods of reduced electricity pricing to undertake cooling loads during peak electricity pricing intervals, culminating in substantial reductions in electricity charges of buildings. Moreover, the strategic reallocation of energy, characterized by a reduced chiller capacity and a corresponding elevation in ice storage system capacity, augments cooling efficiency and diminishes cooling-related electricity expenses. This study offers valuable insights for optimizing and deploying ice storage systems in diverse climatic regions, particularly for shopping malls. As a guiding reference, this paper provides stakeholders with a framework to reasonably apply and adjust ice storage systems, ushering in an era of energy-efficient and environmentally conscious cooling solutions tailored to shopping mall environments.



Citation: Su, F.; Wang, Z.; Yuan, Y.; Song, C.; Zeng, K.; Chen, Y.; Zhang, R. Enhanced Operation of Ice Storage System for Peak Load Management in Shopping Malls across Diverse Climate Zones. *Sustainability* **2023**, *15*, 14759. <https://doi.org/10.3390/su152014759>

Academic Editor: Antonio Caggiano

Received: 30 August 2023

Revised: 7 October 2023

Accepted: 10 October 2023

Published: 11 October 2023



Copyright: © 2023 by the authors. Licensee MDPI, Basel, Switzerland. This article is an open access article distributed under the terms and conditions of the Creative Commons Attribution (CC BY) license (<https://creativecommons.org/licenses/by/4.0/>).

Keywords: ice storage system; shopping malls; system operation; scheme optimization; peak shaving; building simulation

1. Introduction

As society evolves and technology advances, the global energy demand continues to surge, increasing an emission by more than 5% in CO₂ emissions. Carbon emissions

of the building sector account for 1/3 of total carbon emissions. According to the United Nations Environment Program, the building industry should endeavor to reduce energy consumption and greenhouse gas emissions in both developing and developed nations [1]. In 2020, China aimed to reach the carbon peaking and carbon neutrality goals. By 2020, China's operational carbon emissions caused by the building sector maintained an upward trend [2]. In the present context, renewable energy systems are swiftly being used to mitigate the increasingly serious global environmental issue of CO₂ emissions [3]. However, the temporal and spatial instability of clean energy sources often results in the manifestation of the so-called "duck curve" pattern in electricity demand profiles [4]. With increasing generation capacity, this duck curve is transitioning into a canyon curve. This phenomenon has caused concern among many scholars. Energy storage systems can accumulate electricity during low-demand periods and discharge it during peak periods, thus alleviating the pressure on the power grid [5]. Their significance in peak load management and off-peak supply augmentation is progressively becoming more prominent, and their study and development are expanding.

Shopping malls are taken into account for a considerable proportion of total energy consumption [6]. The energy consumption of shopping malls is mainly composed of air conditioning and lighting energy consumption [7]. Furthermore, owing to their substantial pedestrian flow, shopping malls exhibit higher electricity consumption levels during peak hours compared to conventional public buildings. The large discrepancy between peak-to-valley loads illustrates the substantial undeveloped energy-saving potential that energy storage systems can offer when deployed within shopping malls. Yayla et al. [8] developed an artificial intelligence (AI)-based occupant-centric HVAC control mechanism for cooling that continually improves its knowledge to increase energy efficiency in a multi-zone commercial building. Although most shopping malls have adopted intelligent equipment management systems to control refrigeration equipment, allowing them to operate with different strategies based on various environmental parameters and optimizing the use of ice storage systems remains challenging when considering aspects of peak load management and operational strategies across multiple climate zones.

There is extensive research on energy consumption prediction, analysis, and optimization management for shopping malls. Pompei et al. [9] investigated the optimizations of Heating, Ventilation, and Air Conditioning (HVAC) systems for achieving thermal comfort and indoor air quality in shopping malls. Jing et al. [10] proposed an energy-saving diagnosis model for shopping malls based on an improved PSO-SVM neural network, which not only found out the unreasonable situations in the operation of the air-conditioning system but also provided a reference for building energy-saving management and operation. Meanwhile, Zhang et al. [11] took a commercial building in Xi'an as an example, studied the hourly load data of its ice storage cooling system, and used modeling techniques to predict the load of the building.

Thermal energy storage systems find primary application in building air-conditioning systems. As a widely used thermal energy storage form, ice storage system mitigates peak load pressure on the power grid and diminishes the cooling capacity of air-conditioning systems [12]. Compared to chilled water systems and sensible heat storage mechanisms, Chao et al. [13] pointed out that the ice storage system exhibited superior thermal energy density due to its substantial latent heat. This feature indicates that the ice storage system can provide a more efficient and stable energy transmission [14]. Kang et al. [15] found that in buildings employing central air conditioning systems, the integration of ice storage systems with differential peak-to-valley electricity prices can yield cost-saving advantages.

Currently, research on the economic viability of ice storage systems is primarily carried out along the following two dimensions: initial investment and operational expenses. The selection of distinct energy storage tanks [16] and heat exchangers will have a substantial influence on the initial investment. Xu et al. [17] conducted theoretical and experimental research on the ice storage process of coil ice storage air conditioning technology. Heine et al. [18] proposed a recently developed OpenStudio measure for rapid analysis of unitary

thermal storage systems (UTSS). By this metric, the authors evaluated the implementation of UTSS in newly constructed and retrofitted retail buildings equipped with both packaged single-zone air conditioners (PSZAC) and packaged variable air volume (PVAV) systems. Regarding operational expenses, aside from the heat exchanger's intrinsic physical structure, factors include heat transfer efficiency, climate zone, control strategies, and operational schedules. Jannesari et al. [19] conducted a comparative analysis of two heat transfer enhancement methods, specifically, the utilization of thin rings and annular fins around coils. Meng et al. [20] developed an optimization approach for ice storage air conditioning, aiming to minimize both the power purchase cost from the grid and the operational cost of the ice storage air conditioning system. Zou et al. [21] presented a global optimal control strategy to improve the overall energy performance of the system. Control strategies can significantly impact the economic viability of ice storage systems. Gustavo et al. [22] tackled the issue of closed-loop scheduling for a large-scale chiller plant with a thermal energy storage (TES) tank under a d-ahead (DA) electricity price program. In the existing studies, prominent variables for control strategies include system composition, the proportion of chilled water and ice storage systems, chiller capacity, and operational timetables [23]. The prevalent control strategies include chilled water priority mode, ice melting priority mode, and optimized control mode [24,25]. Cui et al. [26] proposed a model-based optimization design methodology to maximize the capacity of active thermal energy storage while minimizing the system's life cycle cost. Allan et al. [27] elaborated on the utilization of piece-wise linear regression and non-linear optimization techniques to ascertain the heat transfer properties of two ice thermal stores with different volumes. Yan et al. [28] introduced a hybrid storage system that fused a seasonal ice storage system reliant on heat pipes with a chilled water storage system, optimizing the operational approach of the configuration. Sanaye et al. [29] introduced two operational modes, namely full operation and partial operation, for ice storage systems, and subsequently compared the costs associated with these modes. Hoseini Rahdar et al. [30] explored peak-to-valley electricity pricing modes in storage systems, assessing their impacts on energy, economics, and the environment. By adjusting ice melting threshold conditions, optimizing the scheduling of the chilled water system [31], and improving the design of the water circulation system [32] it is possible to achieve the most economically efficient optimal operational objectives. Erdemir et al. [33] conducted a thermodynamic and economic analysis of an integrated ice storage system within the air conditioning system of a hypermarket located in Ankara, Turkey. Gholamibozanjani et al. [34] explored the influence of employing a phase change storage system over a brief span (7 days) to enhance cost savings in electricity and heating costs within building models simulated in EnergyPlus, by adopting a model predictive control methodology.

Numerous studies have refined system operation protocols to improve operational strategies and enhance optimization outcomes by creating models, adjusting parameters, and conducting simulations. These studies have also introduced a variety of optimization algorithms based on these models. Tang et al. [35] proposed an optimization framework that integrates a data-driven cooling load prediction model, system physical model, and advanced optimization algorithm and applied it to a district cooling system (DCS) coupled with an ice-based TES in Beijing, China. Hui Cao et al. [36] formulated a similar day algorithm to calibrate and reduce training sample dimensions. J.A. Candanedo et al. [37] proposed a model-based predictive control algorithm designed for building cooling systems that operate under time-varying electricity price profiles. Karl Heine et al. [38] introduced a simulation-optimization workflow that utilized building energy modeling software and mixed-integer linear programming to develop designs and schedules for an integrated refrigeration and thermal storage technology. Xu Song et al. [39] explored a composite ice storage system that combines chilled water and ice storage components. They developed a mathematical model to determine refrigeration capacity and devise daily operational costs for the integrated system. Na Luo et al. [40] gained a comprehensive understanding of the operations of ice storage systems in shopping malls through data-driven analysis and

modeling. They utilized on-site data collected from installed instruments and sensors to calculate system performance. Beghi et al. [41] developed a simulation environment using Matlab/Simulink [42], which integrated continuous and discrete dynamics and accounted for both latent and sensible heat considerations.

Moreover, electricity charging standards in diverse regions directly impact the economic efficiency of ice storage systems [43]. The electricity pricing policies vary across countries and regions with different levels of development. Factors such as interdependencies among different countries and regions, changes in local energy structures [44], and variations in energy demand [45] influence electricity prices. Currently, in various regions of China, time-of-use electricity prices are implemented and further categorized based on the type and scale of electricity consumers.

However, previous studies investigating the economic efficiency viability of ice storage systems have often concentrated on isolated influencing factors, yielding limited insight into the comprehensive and systematic assessment of the synthetic effect of various influencing factors. Additionally, while research on the peak load-shedding capacity of ice storage systems, has primarily centered on individual buildings or specific climate zones, it has relatively underexplored their potential applications of ice storage systems in commercial buildings across diverse climate zones. The lack of rapid urban-scale building modeling tools hinders and restricts the research and discussion on the application effectiveness of ice storage systems in multiple climatic zones. Additionally, the existing developed algorithms and models exhibit limited applicability, failing to support the simulation and computation of multiple urban buildings. Using the baseline models generated by the urban building energy modeling tool named AutoBPS, this study aims to bridge these gaps by considering peak-to-valley electricity pricing, the ratio of chiller capacity (RCC), and system operational schedules to explore the peak shaving capability of ice storage systems in shopping malls situated in different climate regions. Furthermore, it seeks to uncover the relationships and discrepancies among these factors. Simultaneously, this study will undertake a longitudinal analysis spanning various regions within China, enhancing our understanding of the interconnections among these factors, and providing valuable guidance for the implementation of ice storage cooling systems in large commercial buildings. The study's emphasis on peak load management aligns with the core principles of sustainability, as it seeks to optimize energy resources, reduce electricity costs, and minimize its environmental footprint. By shedding light on the potential applications of ice storage systems and their role in peak shaving, this paper contributes valuable insights to the pursuit of sustainable building practices and more environmentally responsible solutions in the realm of energy management and cooling technologies.

The remaining parts of the paper proceed as follows. In Section 2, we provide a detailed introduction to the research methodology of this paper, constructing and simulating the model. In Section 3, we organize and analyze the simulation results of the model, compare the varying effects of ice storage systems in different cities, and conduct an economic analysis. In Sections 4 and 5, we discuss and summarized the significance and limitations of this work.

2. Methodology

The research framework, illustrated in Figure 1, outlines the workflow for the establishment and simulation of an ice storage model. In this study, shopping malls were chosen as representative examples of large public buildings to assess the energy performance of ice storage systems. The initial step was the integration of the ice storage system into a baseline model which included chillers as the cooling source. The baseline models were generated using AutoBPS, a simulation tool that can co-simulate with EnergyPlus (<https://energyplus.net/licensing> (accessed on 1 August 2023)) for urban building energy modeling [46]. Subsequently, the operational strategy was adjusted by modifying the RCC and running schedule according to variational weather conditions. The ice storage system model was established, and its parameters were optimized using OpenStudio

(<https://openstudio.net/> (accessed on 1 August 2023)) based on the input data file (IDF) generated in the previous step. Finally, the energy performance of incorporating the ice storage system was analyzed.

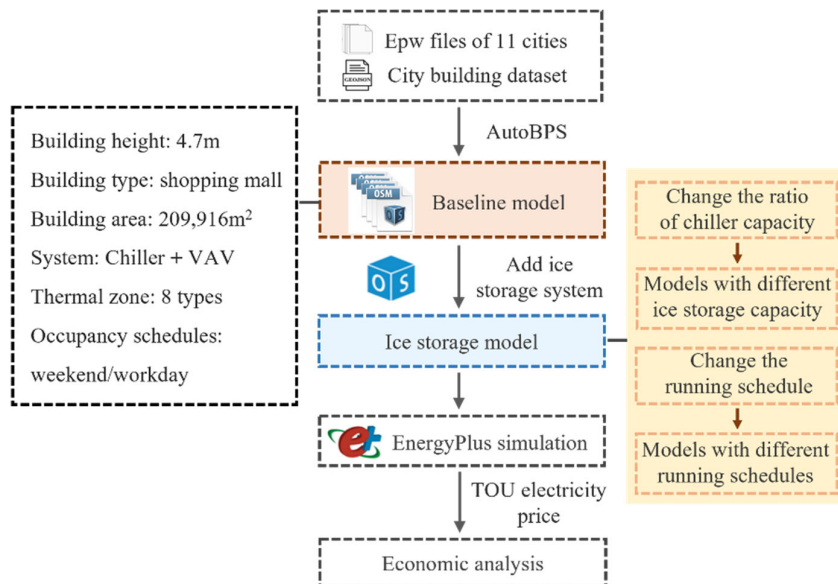


Figure 1. Workflow of establishment and simulation of an ice storage model.

2.1. Baseline Model of the Shopping Mall

Figure 2 presents the building geometry of the baseline model illustrating the baseline shopping mall model, which serves as a prototype and is generated using AutoBPS.

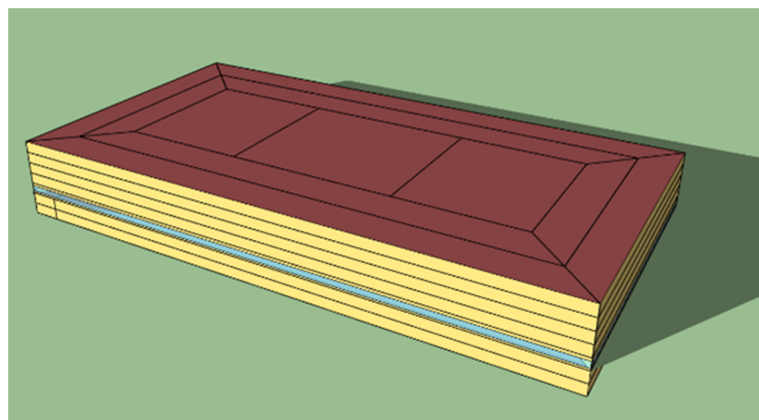


Figure 2. Building geometry of the baseline model.

The parameters of the baseline model are modified through calibration and modeling based on empirical data collected from a specific commercial building in Changsha [47]. This procedure is supported by collecting monthly actual energy consumption data of the commercial buildings, along with basic building parameters like the building envelope structure. Subsequently, this data is input into the urban building modeling tool, AutoBPS-Param, to construct the baseline model of the shopping mall, and Chen et al. used Monte Carlo sampling to calibrate the model results. The range of parameters first refers to the study of Chen et al. [48] and the Chinese national building design standards, including the “GB50189-2005 Energy Efficiency Design Standards for Public Buildings” [49] and “GB50189-2015 Energy Efficiency Design Standards for Public Buildings” [50]. The final models taken into consideration all met the criteria of normalized mean bias error (NMBE) not exceeding 5% and coefficient of variation of the root mean square error (CVRMSE) not

exceeding 15%. These series of comparisons and calibration processes affirm the correctness and effectiveness of our model. The fundamental model acquired through the above-mentioned approach serves as the baseline model for shopping malls in diverse climatic regions nationwide. By integrating weather files of diverse regions into the simulation, we can generate corresponding shopping mall models belonging to specific climate zones.

The building is divided into two underground floors and five above-ground floors, each with a height of 4.7 m. The total area of the building amounts to 209,916 m². The heat transfer coefficient of the external wall and roof is 0.45 W/(m²·K) and 0.4 W/(m²·K), respectively, and the heat transfer coefficient of the outer window is 2.193 W/(m²·K). The highest cooling load index per unit building area above ground is 47.63 W/m². The parameter settings of the baseline model are shown in Table 1.

Table 1. Parameter settings of the baseline model.

Space Type	Occupant per Area Person/m ²	Lighting Power Density W/m ²	Equipment Power Density W/m ²	Area Ratio %
Entertainment	Cinema	0.199	10.0	2.9
	Clothing	0.125	10.0	27.2
	Corrido	0.067	2.5	22.3
	Entertainment	0.199	13.5	3.9
	Restaurant	0.099	9.0	13.6
	Office	0.067	9.0	8.7
	Parking lot	0.049	2.0	16.5
	Supermarket	0.099	11.0	4.9

In the initial design of the building's air conditioning system, the ventilation system employs variable air volume air conditioning terminals, with chillers serving as the cooling source. When the refrigeration system of the baseline model operates under rated conditions, the reference values for fluid temperatures are set as follows: the entering condenser fluid temperature is set at 35 °C as a reference value, and the supply of chilled water is set at 7 °C. The cooling capacity is provided by two chillers concurrently. The capacities of the chillers are set at 1140 tons. The parameter settings of the baseline model system are shown in Table 2. The main functional areas included in the baseline model are restaurants, shops, and supermarkets, which are the primary sources of energy consumption. In the baseline model, their lighting and occupancy schedules are shown in Figure 3.

Table 2. Parameter settings of major components of the baseline model.

	Components	Heat Transfer Coefficient (W/(m ² ·K))	Cooling Load Index (W/m ²)	Number
Building envelope	External wall	0.45		
	Roof	0.4		
	External window	2.193		
	Per unit building area above ground		47.63	
Chillers				2
Pumps	Primary chilled water pump			1
	Second chilled water pump			1
	Condenser water pump			1
Others	Cooling tower			1

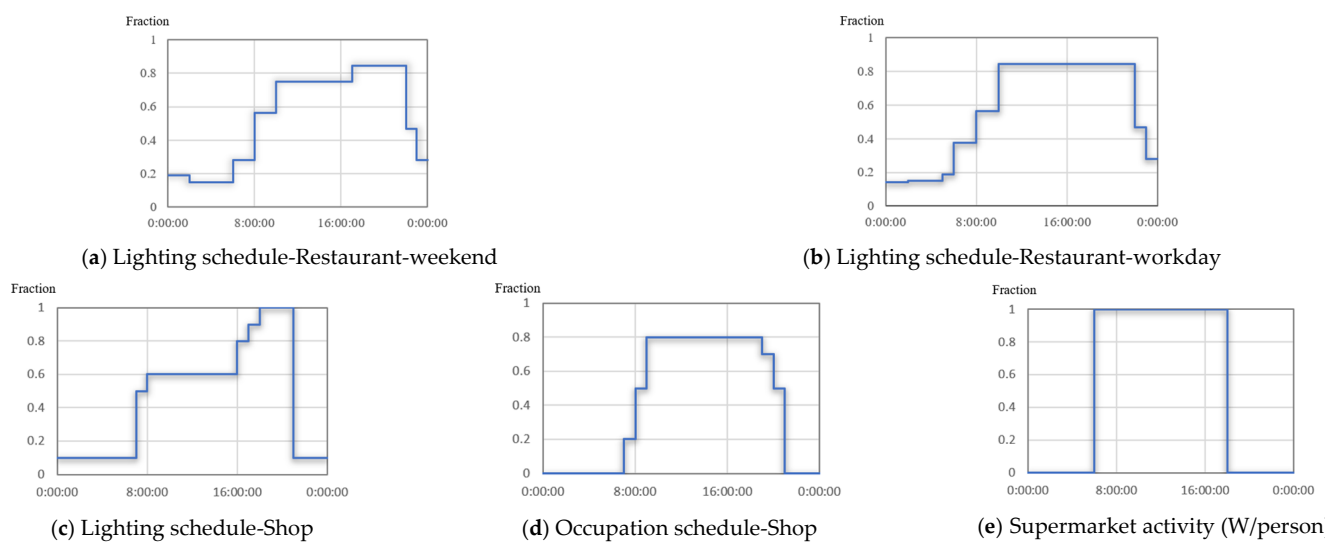


Figure 3. Schedule settings of the baseline model. (The blue line indicates the change in the personnel occupancy rate).

2.2. Establishment of Ice Storage Model

OpenStudio is used to add an ice storage system to the baseline model of the shopping mall. The ice storage models are generated and simulated in EnergyPlus to obtain data such as cooling capacity conversion, cooling power consumption, and unit power consumption of the shopping mall after the integration of the ice storage system. The operating parameters of the ice storage system are modified to make it work under different conditions, and the energy-saving effects of the ice storage system under different operating schemes are compared. This paper mainly investigates the service efficiency of the ice storage system under different parameter settings. The decision variables and available options are shown in Table 3.

Table 3. Variable parameters and available options.

Decision Variables	Option
RCC Running schedule	0.35/0.40/0.50 Ice-priority/TOU schedule

For the modified parameters, the RCC and the running schedule are mainly considered. The change in RCC is primarily achieved by adjusting the variable parameter ‘sizing factor’ of the cooling system’s chiller in OpenStudio. The modification of the running schedule is mainly achieved by altering the temperature variation pattern at the inlet control node of the ice storage tank. By adjusting these two variables, RCC and running schedule, we can obtain ice storage cooling systems with different ice storage capacities and different operating schedules. Under the influence of peak-to-valley electricity prices, this has an impact on the energy consumption of the building’s cooling system.

2.2.1. Addition of Ice Storage System

Based on the baseline model of the shopping mall. OpenStudio is used to add an ice storage system to the baseline model. We take a commercial building located in southern China as an example to study the impact of the ice storage system on energy consumption. The ice storage medium in the loop is set to ethylene glycol with a concentration of 25%, and the temperature of the ethylene glycol is controlled. The lower limit of the temperature range is reduced from 0 °C to –5 °C, the initial cooling capacity of the ice tank is set to 250 GJ, and the outlet temperature is set to 7 °C.

The schematic diagram of the ice storage system added by OpenStudio is illustrated in Figure 4. The cooling system comprises two chillers and two strategically positioned ice tanks within separate branches. At the beginning of the cooling operation, chiller 1 and ice tank 1 are responsible for handling the primary cooling load. If there is insufficient cooling capacity, chiller 2 and ice tank 2, situated in another separate branch, are activated to supplement the cooling demand.

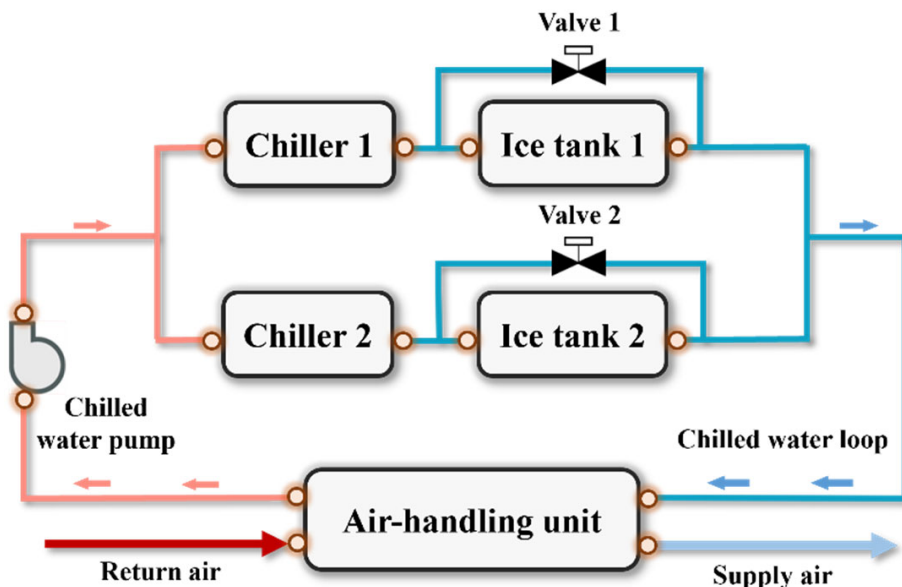


Figure 4. Schematic Diagram of Ice Storage System.

2.2.2. Ice Storage Models for Different Cities: Change the Weather File of the Model

For the 11 cities studied in this paper, cooling loads are different due to their different climatic conditions. Cities with larger cooling loads require longer operating hours and larger capacity for ice storage systems. Still, at the same time, the power consumption of the ice storage system also increases. By changing the weather file of the model in OpenStudio, it is possible to study the energy-saving effect of ice storage systems in cities in different climate zones.

For the 11 cities studied in this article, their climate characteristics are different. In the case of climate characteristics in various regions, they can be represented using Cooling Degree Days (CDD26) and Heating Degree Days (HDD18) as shown in Table 4.

Table 4. Climate Zone Characteristics.

Climate Zone Names	HDD18	CDD26
Severe cold regions	≥ 3800	/
Cold region	2000~3800	>0
Hot summer and cold winter region	1000~2000	>90
Hot Summer and Warm Winter Region	0~1000	>90
Temperate Region	0~1000	0~90

The 11 cities chosen for this study belong to 11 distinct climate zones, 1A, 1B, 1C, and 1D are categorized as severe cold regions, 2A and 2B fall within the cold region, 3A, 3B, and 3C pertain to the hot-summer and cold-winter region. In contrast, 4B and 5A belong to the hot-summer, warm-winter, and temperate regions. Detailed information about the regions where these 11 cities are located is presented in Table 5.

Table 5. Climatic zone characteristics of 11 cities.

City	Thermal Climate Zone		Average Outdoor Temperature		Longitude	Latitude	HDD18	CDD26
	GB50176-2016	ASHRAE Standard 169-2021	21 July	21 January				
Mohe	1A	7	23.1	-41.3	124.12	50.42	6805	4
Heihe	1B	7	25.8	-35.2	127.48	50.25	6310	4
Harbin	1C	7	27.2	-27.8	126.53	45.8	5032	14
Shenyang	1D	5	27.4	-23.1	123.43	41.8	3929	25
Beijing	2A	4	30.2	-10.8	116.4	39.9	2699	94
Taiyuan	2B	5	27.5	-14.9	112.55	37.87	3160	11
Shanghai	3A	3	32.1	-1.9	121.47	32.23	1540	199
Changsha	3B	3	32.9	-1.2	112.93	28.23	1466	230
Chengdu	3C	3	30.1	0.8	104.07	30.67	1344	56
Wuzhou	4B	2	31.1	3.8	111.27	23.48	551	232
Guizhou	5A	3	26.9	-3.1	106.63	26.65	1703	3

2.3. Parameter Adjustment of the Ice Storage System

Among the 11 cities studied, the effects of altering the parameters of Chengdu's model are the most preeminent due to it having the highest cooling load and the highest energy consumption. Therefore, we use Chengdu as an example, study the hourly energy consumption of the baseline model of the shopping mall and the ice storage model on 21 July, and change the control parameters of the ice storage system to observe the changes, to study the effect of different parameters on the ice storage system.

2.3.1. Different Storage Capacity: Change the Sizing Factor of the Chiller

The capacity of the chiller will affect the cold storage capacity of the ice storage system, thereby affecting its power consumption. In OpenStudio, every chiller has a field for "Sizing Factor", which allocates the design load across multiple equipment units with a default value of 1. In this section, manipulating sizing factors allows for load allocation between chillers and ice tanks, as depicted in Formula (1).

$$\text{Sizing factor} = \frac{\text{Cooling load of chiller}}{\text{Total cooling load of all equipment}} \quad (1)$$

Equipment includes chiller 1, chiller 2, ice tank 1, and ice tank 2.

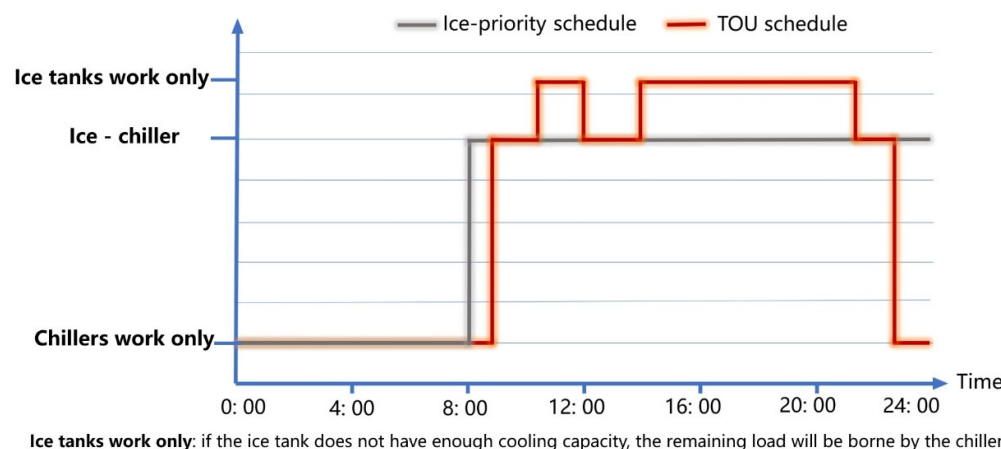
Assuming that the sum of the capacity of the chillers and the ice tanks is 1. When the proportion of the capacity of the chiller is smaller, the proportion of the ice tank is higher, and the cold storage capacity of the chiller is stronger. On the premise of the same operating schedule, the ice storage system with weaker capacity will complete charging faster, but the capacity of cold storage will also be reduced accordingly. The chillers will undertake a higher cooling load when the cooling load is high. By adjusting the sizing factor of the ice storage system within OpenStudio to modify the cold storage capacity and subsequently observing the resulting variation in system cooling power consumption and related data, we can assess the impact of ice storage capacity on the energy-saving potential.

2.3.2. Different Schedules: Change the Running Schedule of the Ice Storage System

Since the chiller and ice tank will simultaneously cool the medium in the circuit, the control of the ice tank's inlet temperature will affect the ice tank's cooling efficiency. When the inlet temperature rises, the chiller will automatically reduce the cooling effect, allowing the ice tank to play a greater role. Therefore, the method of controlling the variation of the inlet temperature in a day is used to control the operation schedule of the ice storage system.

In this paper, two running schedules of the ice storage system are set up, the "Ice-priority" and "TOU schedule". Within these scenarios, under the "Ice-priority" running schedule, the cooling system will give precedence to the ice tank for managing the cooling load during its operation. Conversely, in the case of the "TOU schedule" setting, the cooling system will adapt the operational distribution between the ice storage tank and chiller

according to the variations in peak-to-valley electricity prices throughout the day. The temperature setting of the TOU schedule in OpenStudio is shown in Figure 5. The inlet temperature of the ice tank is 26 °C during the peak electricity price period of the day, −5 °C during the valley value period, and 20 °C during the other period, to charging during the low electricity consumption period and undertaking more cooling capacity during the peak electricity consumption period, thereby reducing the power consumption of the chiller.



Ice tanks work only: if the ice tank does not have enough cooling capacity, the remaining load will be borne by the chiller.

Figure 5. The temperature setting of the TOU schedule.

2.4. Optimization Analysis Using Peak-to-Valley Electricity Price

This study has selected 11 cities in China situated in different climate regions. According to the ‘Unified standard for the design of civil buildings’ [51], various climate zones are categorized using a two-tier regional system. The primary category comprises 7 first-tier climate zones, while the secondary category encompasses 20 second-tier climate zones. The first-tier zones reflect the substantial climatic disparities across the country, while the second-tier zones represent more detailed climatic distinctions within major regions. The 11 cities studied in this study belong to 11 distinct climate zones, 1A, 1B, 1C, and 1D are categorized as severe cold regions, 2A and 2B fall within the cold region, 3A, 3B, and 3C pertain to the hot-summer and cold-winter region. In contrast, 4B and 5A belong to the hot-summer, warm-winter, and temperate regions.

By the above-mentioned methods, the models of the 11 cities studied in this article were individually adjusted parameters and simulated. Their energy consumption and electricity costs were studied to optimize the control strategies of the models. EnergyPlus is used to simulate the ice storage system model under different parameter controls established above, and the output variables of each model are obtained. The economic performance of different models can be studied by applying different electricity price standards in different regions for comparative analysis.

This study investigated the peak-to-valley electricity pricing standards for 11 cities, focusing primarily on commercial electricity consumers within the 1–10 kV voltage range. The survey results show that among the cities, Chengdu has the highest peak power price, and the peak-valley price gap is the largest. The peak price is 1.2621 yuan/kWh, and the valley price is 0.3388 yuan/kWh. The peak electricity price in Taiyuan is the lowest, but the difference between peak and valley electricity prices is the smallest. The peak electricity price is 0.8699 yuan/kWh, and the valley electricity price is 0.3019 yuan/kWh. The detailed electricity price information is presented in Table 6.

Among them, the peak-to-valley period of electricity price is divided as shown in Table 7.

Table 6. Peak-to-valley electricity price.

City	Voltage Level	Electricity Price Policy (Yuan/Degree)		
		Peak Hours	Valley Hours	Flat Hours
1A	Mohe	1–10 kV	1.1270	0.3922
1B	Heihe	1–10 kV	1.1270	0.3922
1C	Harbin	1–10 kV	1.1270	0.3922
1D	Shenyang	1–10 kV	1.0229	0.3635
2A	Beijing	1–10 kV	1.1239	0.5715
2B	Taiyuan	1–10 kV	0.8699	0.3019
3A	Shanghai	1–10 kV	1.0965	0.3427
3B	Changsha	1–10 kV	1.2456	0.3461
3C	Chengdu	1–10 kV	1.2621	0.3388
4B	Wuzhou	1–10 kV	1.1049	0.4028
5A	Guiyang	1–10 kV	0.9680	0.3395

Table 7. The definition of Peak-to-valley period.

Category	Period
Peak hours	11:00–12:00, 14:00–21:00
Valley hours	23:00–7:00 (the next day)
Flat hours	7:00–11:00, 12:00–14:00, 21:00–23:00

In the model output file, the main output data include the cooling capacity conversion of the cooling system, the power consumption of the chiller, the power consumption of the cooling system, the power consumption of the terminal equipment, and so on. This paper primarily focuses on investigating the impact of the ice storage system on the power consumption of the cooling system. Therefore, the main emphasis is placed on analyzing and evaluating the power consumption of the cooling system. According to the results of the above electricity price survey, the economic analysis of the ice storage system is carried out. The calculation method of the operating cost of the ice storage system is as follows: in the output variable files of EnergyPlus, the hourly cooling power consumption of the model is multiplied by the electricity price of the corresponding period and then added to obtain the system operating cost, namely operating costs.

$$W = \sum S_i \times P_i \quad (2)$$

where, S_i is the electricity price corresponding to period i , P_i is the power consumption of the system corresponding to period i .

3. Results

3.1. Validation of the Baseline Model

For the baseline model used in this study, measured data was used to compare and validate the model. A certain commercial building was selected as a case study, and basic building information was collected through on-site visits, and monthly energy consumption data was downloaded from the building management system. The accuracy of the model was verified by comparing the measured monthly electricity consumption data and natural gas usage with the energy consumption data of the baseline model. The coefficient of variation of the root mean square error (CVRMSE) and normalized mean bias error (NMBE) were used as evaluation indicators to reflect the accuracy of the model.

CVRMSE and NMBE are two statistical metrics used to evaluate calibration models. CVRMSE stands for root mean square error coefficient of variation and NMBE stands for normalized mean bias error.

CVRMSE is the ratio of the root mean square error to the mean of the predicted values, usually expressed as a percentage. The smaller the CVRMSE, the higher the predictive accuracy of the model. NMBE is the mean deviation between predicted and actual values,

usually expressed as a percentage. They are calculated using the Formulas (3) and (4). ASHRAE Guideline 14 sets the goal for monthly calibration to be within 15% for CVRMSE and $\pm 5\%$ for NMBE.

$$\text{CVRMSE} = 100\% \times \frac{\left[\sum (y_i - \hat{y}_i)^2 / n \right]^{\frac{1}{2}}}{\bar{y}} \quad (3)$$

$$\text{NMBE} = 100\% \times \frac{\sum (y_i - \hat{y}_i)}{n} \quad (4)$$

where:

y_i is the measured data;

\hat{y} is the simulated data;

\bar{y} is the mean of measured data;

n is the number of the data.

According to Formulas (3) and (4), CVRMSE and NMBE values for energy consumption data and natural gas data were calculated separately. The CVRMSE values for electricity consumption and natural gas are 8.6% and 12.9%, respectively, both less than 15%, while NMBE values are 1.57% and 1.24%, respectively, both less than 5%. These values are within a reasonable range.

The case study building selected is located in Changsha, China, which is a hot summer and cold winter region with high humidity throughout the year. The mall has a floor height of 4.7 m. The first floor of the building has windows, with an east window-to-wall ratio (WWR) of 0.35, south WWR of 0.56, west WWR of 0.35, and north WWR of 0.3. The building area is 209,591 m². The interior space of the building is divided into eight functional types: parking lot, catering, office, cinema, corridor, clothing, supermarket, and entertainment. The area of each functional type is shown in Figures 6 and 7.

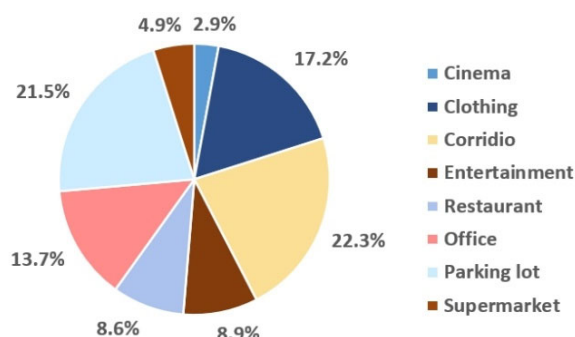


Figure 6. Area of each function type (measured data).

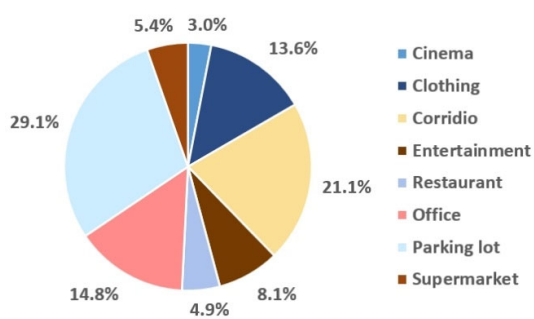


Figure 7. Area of each function type (baseline model).

After summarizing and compiling the monthly electricity and natural gas usage data for the shopping mall, it can be seen that the electricity consumption is higher in summer, with a maximum unit area electricity consumption index of 15.79 kWh/m² in

August, while natural gas usage is highest in January at 0.02178 GJ/m^2 . Compared with the simulated electricity consumption and natural gas usage data of the baseline model, which are summarized in Figures 8 and 9. The figures show the monthly energy consumption change curves for measured and simulated data, respectively.

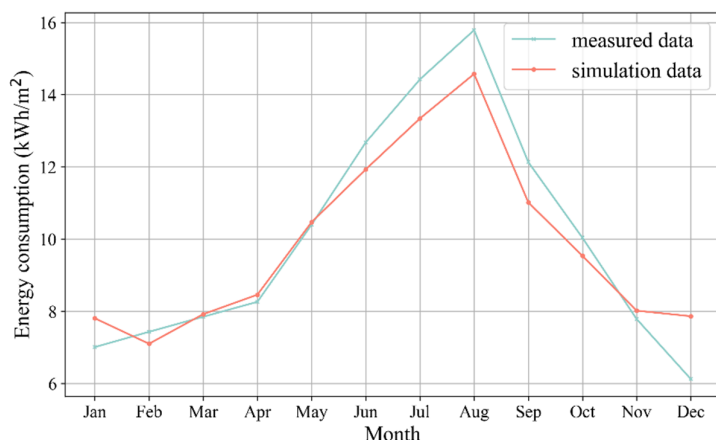


Figure 8. Monthly electrical energy consumption.

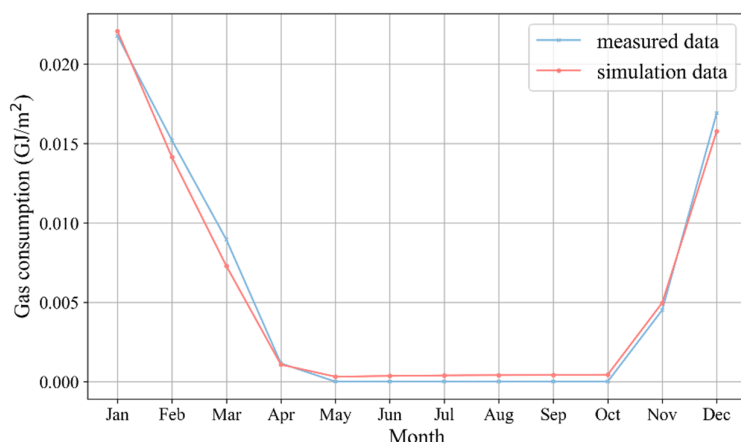


Figure 9. Monthly natural gas consumption.

3.2. Simulation Results of Baseline Models of Different Cities

For the 11 cities studied, the corresponding regional weather file is added to the baseline model of their shopping malls in OpenStudio, and EnergyPlus is used to simulate the models above. The energy consumption of the cooling system of the baseline model in each region can be obtained.

Referring to the energy consumption of unit area in a year except for the heating index of general public buildings, which is $60\text{--}110 \text{ kWh}/(\text{m}^2\cdot\text{a})$ [52], the annual energy consumption of each model of 11 cities is calculated and converted into the energy consumption of unit area except heating. The results are shown in Figure 10.

One important point to note is that, due to Guiyang having a longer cooling season and a lower peak load, compared to Taiyuan, despite Guiyang having a cooler climate, the values of non-heating energy consumption indicators are higher.

Two chillers are working at the same time in the refrigeration system of the model. The main cooling load is borne by chiller 1. Because the Chengdu model demonstrates the highest cooling load among all the models under study, the array of metrics related to refrigeration achieves an enhanced level of representational significance. Consequently, the Chengdu model is herein selected as the exemplar for illustration. Figure 11 shows the monthly energy consumption of the baseline model of Chengdu. Among them, (a) shows

the monthly cooling power consumption of the baseline model in Chengdu City, and (b) shows the COP of two chillers in the air conditioning system. It was found that the COP of the chillers will reach the maximum in July and August when the cooling load is the highest. The COP of chiller 1 in each model was calculated. The results are shown in Figure 12. Compared to other periods, the COP of chiller 1 is higher during periods of higher cooling load throughout the year.

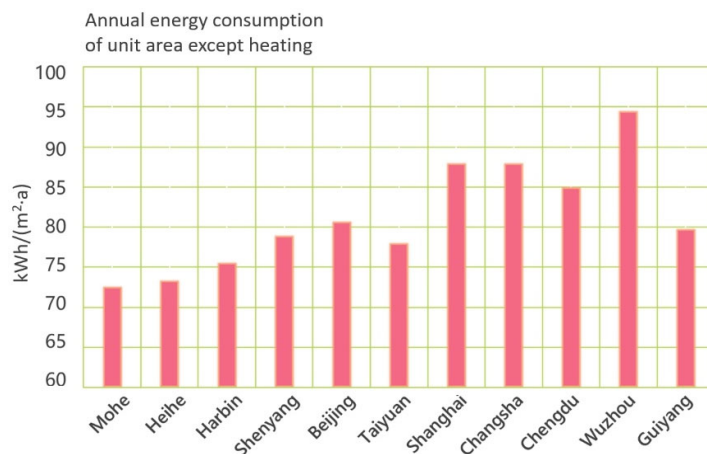


Figure 10. Annual energy consumption of unit area except for heating.

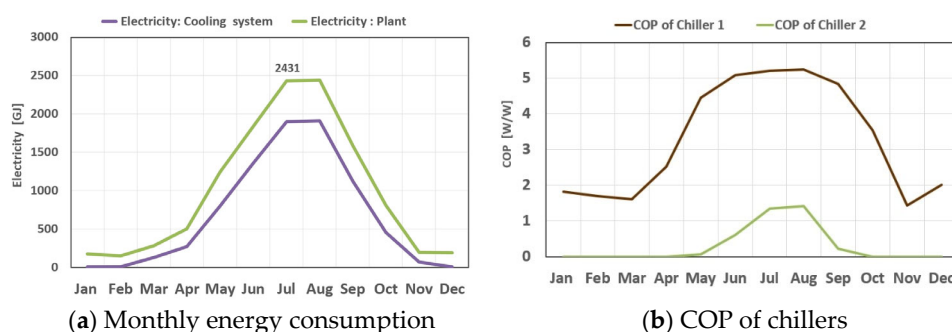


Figure 11. Energy consumption of the Chengdu model.

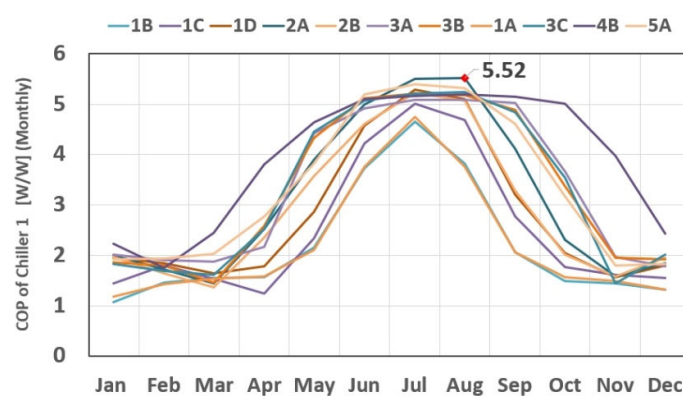


Figure 12. The annual variation of Chiller 1's COP.

From the preliminary simulation results, the peak power consumption of the cooling system of the baseline model appears in July and August, and the minimum value appears in January and February. The energy consumption of these models decreases with the increase of latitude in the region, which is consistent with the actual situation that the lower the latitude of the city, the larger the demand for cooling capacity.

3.3. Simulation Results of Ice Storage Model

The ice storage system's initial operational schedule is configured as the "Ice-priority" schedule, and the initial allocation of chiller capacity is set at 0.35. To integrate the ice storage systems into the baseline model, we monitor the hourly fluctuations of the chiller's Coefficient of Performance (COP) on 21 July before and after this integration. This study draws attention to 11 cities located within five diverse climate zones in China. Among these, the following four cities were specifically chosen as representatives: Mohe, Beijing, Changsha, and Guiyang. The primary objective is to conduct a comprehensive hour-by-hour analysis of the operational dynamics of refrigeration systems in these four cities, specifically on 21 July, a day characterized by exceptionally high cooling load demands. The findings are visually presented in Figures 13–16. It is evident that after adding the ice storage system, the chiller unit will experience long periods of inactivity. During these intervals, the ice storage system entirely supports the cooling load. At the same time, during the remaining periods, it collaborates with the ice storage system concurrently, thus facilitating the achievement of peak-shaving and valley-filling energy consumption effects. Furthermore, as the cooling demand intensifies in urban areas, the chiller's downtime is reduced. This phenomenon can be attributed to the frequent collaboration between the chiller and the local ice storage system, driven by the increasing demand for cooling requirements.

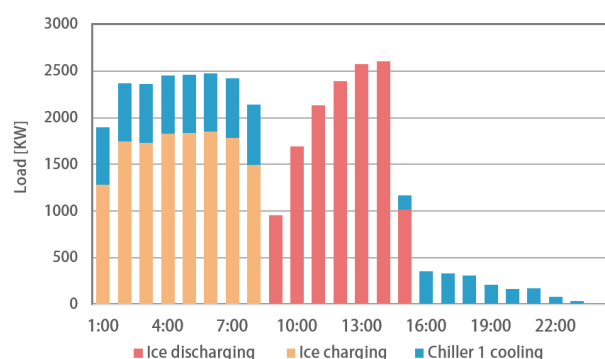


Figure 13. Operational strategies on a high cooling load day of the Mohe model.

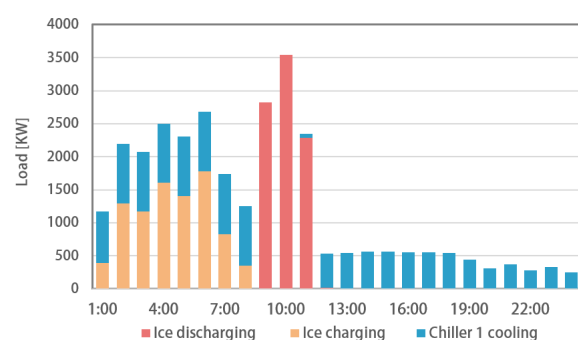


Figure 14. Operational strategies on a high cooling load day of the Beijing model.

The ice storage system is added to the baseline model in different cities and simulated to obtain the energy consumption data of the model before and after the addition. The energy consumption data before and after the addition of the ice storage system is subtracted, which is the energy consumption saved by the ice storage system. By calculating the annual electricity cost using the provided data, the cost savings in electricity expenses can be determined for different cities upon the implementation of ice storage systems. The annual electricity cost calculation results of the 11 models are summarized in Figure 17.

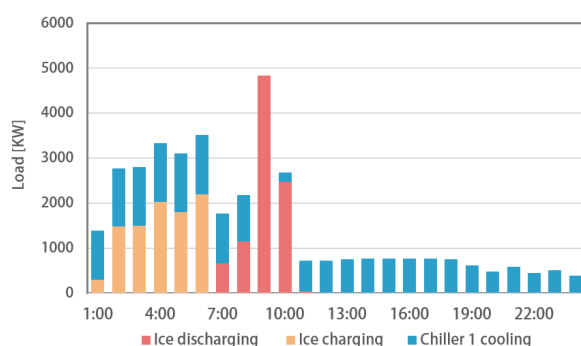


Figure 15. Operational strategies on a high cooling load day of the Changsha model.

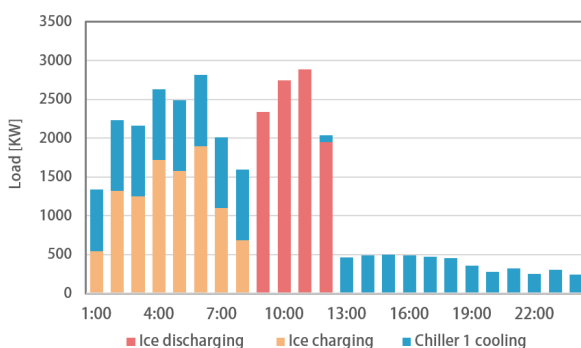


Figure 16. Operational strategies on a high cooling load day of the Guiyang model.

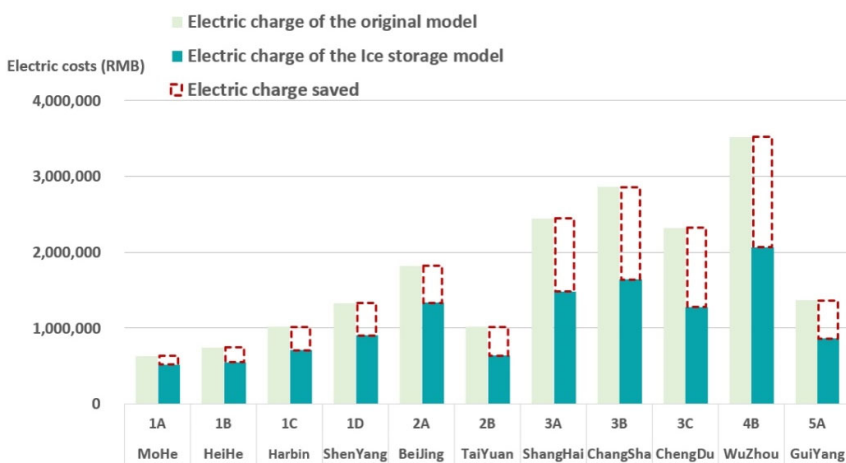


Figure 17. Annual electricity cost of the models.

Among them, the Chengdu ice storage model has the largest reduction in electricity bills. A total of 1,043,120 yuan in electricity costs will be saved each year, a decrease of 44.92% compared with the baseline model. While the baseline model in Wuzhou has the highest electricity cost, after adding the ice storage system, the system can save the highest amount of electricity in the whole year, which is 1,451,263 yuan. The electricity cost savings in Mohe after adding the ice storage model account for the smallest proportion of the electricity cost of the meta-model, which is 17.37%, saving 521,314 yuan per year. The simulation results of other models are summarized in Table 8.

Table 8. Electricity cost of the 11 models with different cooling systems.

City	Climate Zone	Electric Costs of the Baseline Model/Yuan	Electric Costs of the Ice Storage Model/Yuan	Electric Costs Saved/Yuan	Variation
Mohe	1A	630,905	521,314	109,590	17.37%
Heihe	1B	746,877	548,283	198,593	26.59%
Harbin	1C	1,014,725	709,499	305,225	30.08%
Shenyang	1D	1,330,321	901,650	428,670	32.22%
Beijing	2A	1,818,894	1,332,607	486,286	26.74%
Taiyuan	2B	1,015,795	637,805	377,989	37.21%
Shanghai	3A	2,446,728	1,480,026	966,702	39.51%
Changsha	3B	2,858,214	1,642,792	1,215,422	42.52%
Chengdu	3C	2,322,064	1,278,944	1,043,120	44.92%
Wuzhou	4B	3,518,594	2,067,331	1,451,263	41.25%
Guizhou	5A	1,365,668	861,824	503,844	36.89%

3.4. Optimization Results of the Control Parameters for the Case Model

3.4.1. Changing the Proportion of Chiller Capacity

The initial setting of the ice storage system stipulates that the operating schedule is the “Ice-priority” schedule, and the sizing factor of the chiller is set to 0.35, 0.4, and 0.5 separately for simulation. The simulation results are shown in Figure 18.

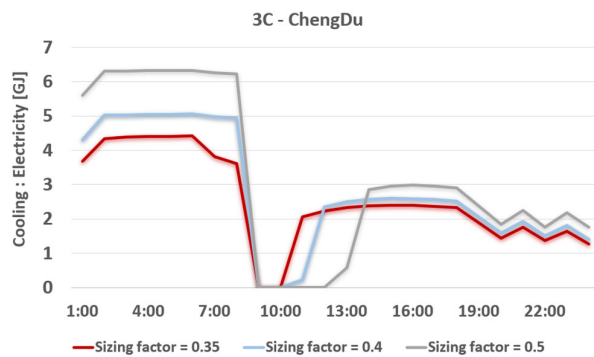


Figure 18. Energy consumption of the chillers with different sizing factors.

The simulation results of the model with different sizing factors in Chengdu are shown in Table 9. When the proportion of chiller capacity decreases, the ice storage system will undertake more cooling load, and the electricity costs of the cooling system will also drop significantly. The proportion of chiller capacity is 0.35, compared with the ratio of 0.5, the electricity costs on a typical design day will be reduced by 13.41%. However, when the chiller’s capacity is lower than 0.35, the electricity costs of the cooling systems do not decrease significantly. Considering that the load of the chiller is too small in this situation, the initial investment in the ice storage system may increase, which will lead to an increase in the total cost and improve the economic efficiency of the system.

Table 9. Simulation results of the model with different sizing factors in Chengdu.

	Sizing Factor = 0.3	Sizing Factor = 0.4	Sizing Factor = 0.5
Electric costs [yuan]	12,619.4	13,537	14,573.9
Cooling Electricity [GJ]	61	67.6	77.1

3.4.2. Changing the Schedule of the Ice Storage System

In the initial configuration of the ice storage system, the chiller’s capacity ratio is specified at 0.35. The simulation involves the use of two kinds of schedules. The simulation results are shown in Figure 19.

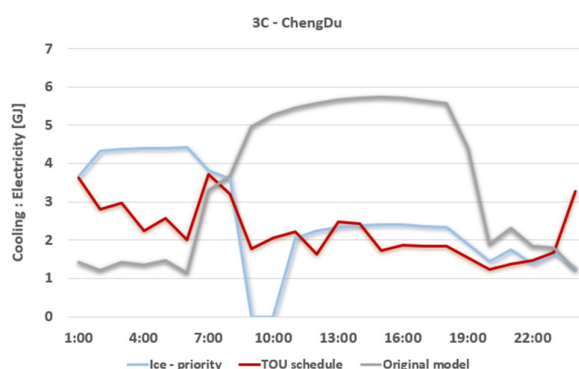


Figure 19. Energy consumption of the chillers with different running schedules.

The graph illustrates that the cooling electricity consumption curve of the baseline model exhibits relatively high values during the peak cooling load period within a day, with a maximum peak of 5.74 GJ occurring at 15:00. After the incorporation of the ice storage system and operating it under the TOU schedule, it demonstrates a more uniform energy consumption pattern in contrast to the ‘Ice-priority’ schedule. Analyzing the simulation results of the ice storage system under two distinct operation schedules, it is observed that when the system operates based on the ‘TOU schedule,’ it enables charging during periods of low power consumption and working during the peak power consumption period. Actively undertaking more cooling loads during different periods can reasonably use the fluctuation characteristics of electricity prices in a day to work so that the system’s electricity consumption costs can be reduced during peak periods, thereby achieving the effect of peak-shaving and valley-filling electricity consumption. Compared to the baseline model’s electricity costs on 21 July, the electricity costs of the model running according to the ‘Ice-priority’ schedule will decrease by 45.97%, while the electricity costs of the model running under the ‘TOU schedule’ will decrease by 50.83%.

3.5. Optimization Results of Model Operation Schemes for Each City

Based on the research above, we can derive a preliminary conclusion: applying an ice storage system in regions with a substantial cooling load offers a greater potential for energy conservation. Furthermore, the effective utilization of peak-to-valley electricity pricing can significantly reduce energy consumption. Adopting the methodology described above, the parameters for the 11 cities examined in this study were adjusted and simulated. As a result, an operational control strategy for the ice storage system was developed, according to each city’s specific climate zone.

3.5.1. Optimizing Chiller Capacity

When the proportion of chiller capacity decreases, the ice storage system will undertake more cooling load, and the cooling power consumption of the system will also decrease accordingly. Nonetheless, it’s important to note that the chiller’s capacity should be raised. This method might lead to an augment in the initial investment of the ice storage system, subsequently raising the overall cost and potentially impacting the energy performance of the system. For the 11 cities studied, their different peak-to-valley flat electricity price structures will also impact the effect of chiller capacity. From the analysis above, it can be observed that there is a linear relationship between the electricity cost of the ice storage system and the sizing factor. Therefore, for the research conducted on the models of other cities, the scenario where the sizing factor equals 0.4 can be excluded. Comparing the two cases where the sizing factor of the chiller is 0.35 and 0.5, the most significant decrease in electricity costs is the ice storage system of Chengdu, and in cities apart from Chengdu, when the sizing factor of the chiller is 0.35, the effect of saving electricity costs is better. Except for Chengdu, the models of Changsha and Wuzhou demonstrate more preeminent effects when altering the sizing factor. In comparison to the baseline model,

they can achieve electricity cost savings of 45.52% and 41.25%, respectively. The results are summarized in Table 10.

Table 10. Simulation results of models with different sizing factors.

City	Climate Zone	Electric Costs Saved/Yuan		Variation	
		Sizing Factor = 0.35	Sizing Factor = 0.5	Sizing Factor = 0.35	Sizing Factor = 0.5
Mohe	1A	109,590	1022	17.37%	0.16%
Heihe	1B	198,593	109,025	26.59%	14.60%
Harbin	1C	305,225	202,353	30.08%	19.94%
Shenyang	1D	428,670	333,529	32.22%	25.07%
Beijing	2A	486,286	298,630	26.74%	16.42%
Taiyuan	2B	377,989	327,003	37.21%	32.19%
Shanghai	3A	966,702	931,048	39.51%	38.05%
Changsha	3B	1,215,422	1,149,862	42.52%	40.23%
Chengdu	3C	1,043,120	1,086,317	44.92%	46.78%
Wuzhou	4B	1,451,263	1,348,566	41.25%	38.33%
Guiyang	5A	503,844	416,362	36.89%	30.49%

3.5.2. Optimizing the Operation Schedule

During the 12 months of the year, the running schedules of the ice storage systems in the 11 cities studied in this paper were adjusted and simulated, and the obtained data were substituted into the calculations according to Formula (2). When the ice storage system operates according to the ‘TOU schedule’, the annual electricity costs will be reduced to varying degrees. The results obtained are summarized in Table 11.

Table 11. Simulation results of models with different running schedules.

City	Climate Zone	Electric Costs Saved/Yuan		Variation	
		Ice-Priority	TOU Schedule	Ice-Priority	TOU Schedule
Mohe	1A	109,590	154,782	17.37%	24.53%
Heihe	1B	198,593	234,978	26.59%	31.46%
Harbin	1C	305,225	363,656	30.08%	35.84%
Shenyang	1D	428,670	528,593	32.22%	39.73%
Beijing	2A	486,286	575,912	26.74%	31.66%
Taiyuan	2B	377,989	436,452	37.21%	42.97%
Shanghai	3A	966,702	1,166,709	39.51%	47.68%
Changsha	3B	1,215,422	1,385,999	42.52%	48.49%
Chengdu	3C	1,043,120	1,242,884	44.92%	53.52%
Wuzhou	4B	1,451,263	1,645,692	41.25%	46.77%
Guiyang	5A	503,844	611,538	36.89%	44.78%

The simulation results revealed a significant correlation: the closer a city is to the equator, namely a lower latitude, the higher the cooling load becomes. Furthermore, the potential of applying ice storage systems is larger and results in more prominent economic efficiency.

In addition, the greater the difference between peak and valley electricity prices, the better the energy-saving effect of the ice storage system. Among these 11 cities, Chengdu has the largest difference in peak-to-valley electricity prices, and the cooling load in the cooling season is relatively large. Hence, the ice storage system applied in Chengdu has the best effect in saving electricity costs and has the considerable potential of applying ice storage systems.

4. Discussion

This article has studied the enhanced operation of ice storage systems for peak load management in shopping malls across diverse climate zones. The research aimed to

optimize the economic performance and cooling efficiency of these systems by considering the unique electricity pricing frameworks of different cities. The findings of the study provide valuable insights for stakeholders involved in the deployment and operation of ice storage systems in shopping malls. However, there are several aspects worth discussing or improving.

- (1) One of the key observations from the research is the significant peak-shaving and valley-filling effects observed in regions characterized by lower latitudes and substantial cooling loads. Ice storage systems effectively reduce peak electricity demand and shift cooling loads to off-peak periods in such climatic conditions. By leveraging the temporal dynamics of TOU power pricing, a finely calibrated operational schedule for the ice storage system was devised, resulting in substantial reductions in model electricity charges.
- (2) The study highlights the importance of ice storage capacity and operational schedules in influencing economic viability and cooling efficiency. Strategic reallocation of resources, such as reducing chiller capacity and increasing ice storage system capacity, enhances cooling efficiency and reduces cooling-related electricity expenses. Optimizing the capacity balance between chiller systems and ice storage systems improves overall performance.
- (3) In this paper, the baseline model is verified by comparing the measured energy consumption data. Although the evaluation indexes are in a reasonable range, the model can actually be made to meet the requirements by using other combinations of parameters, for example, using different combinations of cooling systems and building envelopes, etc. In the future research, more real cases of ice storage systems should be researched, and parameters should be limited to a more precise range to get a baseline model with higher accuracy and credibility, and a discussion should be carried out on the basis of which, so as to better research on the future application of phase-change thermal storage systems in energy saving of buildings.
- (4) It is important to acknowledge the limitations and difficulties faced during the study. The research focused specifically on shopping malls, and the findings may not directly apply to other types of buildings or facilities. Additionally, the study assumed ideal conditions and did not consider factors such as equipment reliability, maintenance costs, and implementation challenges that may arise in real-world scenarios. Future research should address these limitations by conducting field studies and considering a broader range of building types.
- (5) The primary focus of this study is on the simulation and operational optimization of ice storage systems in multi-climate zones at the urban scale. Additionally, the research includes an economic analysis and discussion of the model's output results. However, there is a lack of thorough validation and error analysis of the optimized model's results. The absence of real-world building data that closely aligns with the model has posed challenges for result validation. In future research, further study of the model's result accuracy to calibrate and refine additional details of the model will be developed, which will allow for a more comprehensive validation of the model's optimization outcomes.

Furthermore, the research could benefit from exploring additional control strategies for ice storage systems. The study primarily focused on chilled water priority mode, ice melting priority mode, and optimized control mode. Investigating other control strategies and evaluating their performance in different climate zones could provide further insights into maximizing the economic viability and cooling efficiency of ice storage systems.

Overall, this article demonstrates the optimization and deployment of ice storage systems in shopping malls across diverse climate zones. It emphasizes the importance of considering electricity pricing frameworks, capacity balance, and operational schedules in achieving economic performance and cooling efficiency. However, further research is needed to address limitations, explore alternative control strategies, and validate the findings in real-world scenarios. By continuing to investigate and refine ice storage system

operation, stakeholders can make informed decisions and effectively utilize this sustainable cooling solution in various climatic regions.

5. Conclusions

In this study, we extensively examined the development and economic evaluation of ice storage system models in 11 diverse Chinese cities' shopping malls. We crafted precise operational strategies tailored to each city's unique climate conditions. Our approach involved integrating ice storage systems into various shopping mall models in distinct regions and conducting comprehensive simulations.

The results reveal the substantial impact of ice storage systems on reducing peak electricity costs and meeting cooling demands in shopping malls, particularly in lower latitude areas with higher cooling needs. These improvements in economic performance were most pronounced in Chengdu, where cooling electricity expenses saw the most significant reduction due to the incorporation of ice storage systems.

We also highlight the importance of ice storage capacity and operational schedules in enhancing the system's economic viability and cooling efficiency. Skillful adjustment of the ice tank's inlet temperature during peak-to-valley electricity pricing fluctuations enables the system to charge during low-price periods and provide cooling during peak-price intervals, resulting in significant cost savings. The implementation of a 'TOU schedule' notably reduced electricity charges in the Chengdu model. Additionally, our study underscores that reducing the chiller's sizing factor increases the ice storage system's capacity to handle cooling loads, leading to decreased electricity charges to some extent. This effect is particularly prominent in the shopping malls in cities with higher cooling demands.

In conclusion, our comprehensive analysis of ice storage system models across diverse climatic regions in China offers valuable insights for optimized system implementation. Our research emphasizes the importance of tailored operational schedules, adjustments to ice storage capacity, and chiller sizing optimization to enhance economic performance and cooling efficiency. These findings provide a valuable resource for practitioners and decision makers seeking sustainable and cost-effective cooling solutions in shopping mall environments.

Author Contributions: Writing—original draft, F.S.; Writing—review & editing, Z.W., Y.Y., C.S., K.Z. and R.Z.; Visualization, K.Z.; Supervision, Y.C. All authors have read and agreed to the published version of the manuscript.

Funding: This research was funded by Hunan University, China, through the Course Development Program of "Artificial Intelligence in Built Environment". It was supported by research start-up funds for newly recruited teachers at Hunan University, aiming to "Develop an Urban Energy System Modeling and Simulation Platform to Support Building Energy Efficiency Improvement".

Institutional Review Board Statement: Not applicable.

Informed Consent Statement: Not applicable.

Data Availability Statement: Not applicable.

Conflicts of Interest: The authors declare no conflict of interest.

References

- Asensio, O.I.; Delmas, M.A. The effectiveness of US energy efficiency building labels. *Nat. Energy* **2017**, *2*, 17033. [[CrossRef](#)]
- Hu, S.; Zhang, Y.; Yang, Z.; Yan, D.; Jiang, Y. Challenges and opportunities for carbon neutrality in China's building sector—Modelling and data. *Build. Simul.* **2022**, *15*, 1899–1921. [[CrossRef](#)]
- IEA—International Energy Agency. Available online: <https://www.iea.org/reports/%20global-energy-review-2021> (accessed on 9 August 2023).
- Wong, L.A.; Ramachandaramurthy, V.K.; Walker, S.L.; Ekanayake, J.B. Optimal Placement and Sizing of Battery Energy Storage System Considering the Duck Curve Phenomenon. *IEEE Access* **2020**, *8*, 197236–197248. [[CrossRef](#)]
- Killer, M.; Farrokhseresht, M.; Paterakis, N.G. Implementation of large-scale Li-ion battery energy storage systems within the EMEA region. *Appl. Energy* **2020**, *260*, 114166. [[CrossRef](#)]
- Curto, D.; Franzitta, V.; Longo, S.; Montana, F.; Riva Sanseverino, E. Investigating energy saving potential in a big shopping center through ventilation control. *Sustain. Cities Soc.* **2019**, *49*, 101525. [[CrossRef](#)]

7. Catrini, P.; Curto, D.; Franzitta, V.; Cardona, F. Improving energy efficiency of commercial buildings by Combined Heat Cooling and Power plants. *Sustain. Cities Soc.* **2020**, *60*, 102157. [[CrossRef](#)]
8. Yayla, A.; Swierczewska, K.S.; Kaya, M.; Karaca, B.; Arayici, Y.; Ayozen, Y.E.; Tokdemir, O.B. Artificial Intelligence (AI)-Based Occupant-Centric Heating Ventilation and Air Conditioning (HVAC) Control System for Multi-Zone Commercial Buildings. *Sustainability* **2022**, *14*, 16107. [[CrossRef](#)]
9. Pompei, L.; Nardeschia, F.; Viglianese, G.; Rosa, F.; Piras, G. Towards the Renovation of Energy-Intensive Building: The Impact of Lighting and Free-Cooling Retrofitting Strategies in a Shopping Mall. *Buildings* **2023**, *13*, 1409. [[CrossRef](#)]
10. Jing, W.; Yu, J.; Luo, W.; Li, C.; Liu, X. Energy-saving diagnosis model of central air-conditioning refrigeration system in large shopping mall. *Energy Rep.* **2021**, *7*, 4035–4046. [[CrossRef](#)]
11. Zhang, W.; Yu, J.; Zhao, A.; Zhou, X. Predictive model of cooling load for ice storage air-conditioning system by using GBDT. *Energy Rep.* **2021**, *7*, 1588–1597. [[CrossRef](#)]
12. Soler, M.S.; Sabaté, C.C.; Santiago, V.B.; Jabbari, F. Optimizing performance of a bank of chillers with thermal energy storage. *Appl. Energy* **2016**, *172*, 275–285. [[CrossRef](#)]
13. Chao, J.; Xu, J.; Bai, Z.; Wang, P.; Wang, R.; Li, T. Integrated heat and cold storage enabled by high-energy-density sorption thermal battery based on zeolite/MgCl₂ composite sorbent. *J. Energy Storage* **2023**, *64*, 107155. [[CrossRef](#)]
14. Boulaktout, N.; Mezaache, E.H.; Teggar, M.; Arıcı, M.; Ismail, K.A.R.; Yıldız, Ç. Effect of Fin Orientation on Melting Process in Horizontal Double Pipe Thermal Energy Storage Systems. *J. Energy Resour. Technol.* **2021**, *143*, 070904. [[CrossRef](#)]
15. Kang, Z.; Wang, R.; Zhou, X.; Feng, G. Research Status of Ice-storage Air-conditioning System. *Procedia Eng.* **2017**, *205*, 1741–1747. [[CrossRef](#)]
16. Seitz, M.; Johnson, M.; Hübner, S. Economic impact of latent heat thermal energy storage systems within direct steam generating solar thermal power plants with parabolic troughs. *Energy Convers. Manag.* **2017**, *143*, 286–294. [[CrossRef](#)]
17. Xu, X.; Chang, C.; Guo, X.; Zhao, M. Experimental and Numerical Study of the Ice Storage Process and Material Properties of Ice Storage Coils. *Energies* **2023**, *16*, 5511. [[CrossRef](#)]
18. Heine, K.; Cesar Tabares-Velasco, P.; Deru, M. Energy and cost assessment of packaged ice energy storage implementations using OpenStudio Measures. *Energy Build.* **2021**, *248*, 111189. [[CrossRef](#)]
19. Jannesari, H.; Abdollahi, N. Experimental and numerical study of thin ring and annular fin effects on improving the ice formation in ice-on-coil thermal storage systems. *Appl. Energy* **2017**, *189*, 369–384. [[CrossRef](#)]
20. Meng, L.; Chen, L.; Jiang, T.; Xu, F.; Yao, X.; Hao, L.; Yang, S. Air conditioning dispatching and economic analysis of ice storage in urban power grid. *IOP Conf. Ser. Earth Environ. Sci.* **2019**, *295*, 052006. [[CrossRef](#)]
21. Zou, W.; Sun, Y.; Gao, D.; Zhang, X. Globally optimal control of hybrid chilled water plants integrated with small-scale thermal energy storage for energy-efficient operation. *Energy* **2023**, *262*, 125469. [[CrossRef](#)]
22. Campos, G.; Liu, Y.; Schmidt, D.; Yonkoski, J.; Colvin, D.; Trombly, D.M.; El-Farra, N.H.; Palazoglu, A. Optimal real-time dispatching of chillers and thermal storage tank in a university campus central plant. *Appl. Energy* **2021**, *300*, 117389. [[CrossRef](#)]
23. Kamal, R.; Moloney, F.; Wickramaratne, C.; Narasimhan, A.; Goswami, D.Y. Strategic control and cost optimization of thermal energy storage in buildings using EnergyPlus. *Appl. Energy* **2019**, *246*, 77–90. [[CrossRef](#)]
24. Arcuri, B.; Spataru, C.; Barrett, M. Evaluation of ice thermal energy storage (ITES) for commercial buildings in cities in Brazil. *Sustain. Cities Soc.* **2017**, *29*, 178–192. [[CrossRef](#)]
25. Li, H.; Wang, S. Model-based multi-objective predictive scheduling and real-time optimal control of energy systems in zero/low energy buildings using a game theory approach. *Autom. Constr.* **2020**, *113*, 103139. [[CrossRef](#)]
26. Cui, B.; Gao, D.; Xiao, F.; Wang, S. Model-based optimal design of active cool thermal energy storage for maximal life-cycle cost saving from demand management in commercial buildings. *Appl. Energy* **2017**, *201*, 382–396. [[CrossRef](#)]
27. Allan, J.; Croce, L.; Dott, R.; Georges, G.; Heer, P. Calculating the heat loss coefficients for performance modelling of seasonal ice thermal storage. *J. Energy Storage* **2022**, *52*, 104528. [[CrossRef](#)]
28. Yan, C.; Shi, W.; Li, X.; Zhao, Y. Optimal design and application of a compound cold storage system combining seasonal ice storage and chilled water storage. *Appl. Energy* **2016**, *171*, 1–11. [[CrossRef](#)]
29. Sanaye, S.; Hekmatian, M. Ice thermal energy storage (ITES) for air-conditioning application in full and partial load operating modes. *Int. J. Refrig.* **2016**, *66*, 181–197. [[CrossRef](#)]
30. Hoseini Rahdar, M.; Emamzadeh, A.; Ataei, A. A comparative study on PCM and ice thermal energy storage tank for air-conditioning systems in office buildings. *Appl. Therm. Eng.* **2016**, *96*, 391–399. [[CrossRef](#)]
31. Al-Aali, I.; Narayanaswamy, A.; Modi, V. A novel algorithm for optimal equipment scheduling and dispatch of chilled water systems with ice thermal storage. *Energy Build.* **2022**, *274*, 112422. [[CrossRef](#)]
32. Zhou, R.; Tu, P.; Zhang, H. Performance improvement of alternate temperature systems with ice storage-based internal water loop. *Energy Build.* **2019**, *204*, 109521. [[CrossRef](#)]
33. Altuntop, N.; Çengel, Y.A. Experimental investigation on the effect of ice storage system on electricity consumption cost for a hypermarket. *Energy Build.* **2021**, *251*, 111368. [[CrossRef](#)]
34. Gholamibozanjani, G.; Tarragona, J.; Gracia, A.d.; Fernández, C.; Cabeza, L.F.; Farid, M.M. Model predictive control strategy applied to different types of building for space heating. *Appl. Energy* **2018**, *231*, 959–971. [[CrossRef](#)]
35. Tang, H.; Yu, J.; Geng, Y.; Liu, X.; Lin, B. Optimization of operational strategy for ice thermal energy storage in a district cooling system based on model predictive control. *J. Energy Storage* **2023**, *62*, 106872. [[CrossRef](#)]

36. Cao, H.; Lin, J.; Li, N. Optimal control and energy efficiency evaluation of district ice storage system. *Energy* **2023**, *276*, 127598. [[CrossRef](#)]
37. Candanedo, J.A.; Dehkordi, V.R.; Stylianou, M. Model-based predictive control of an ice storage device in a building cooling system. *Appl. Energy* **2013**, *111*, 1032–1045. [[CrossRef](#)]
38. Heine, K.; Tabares-Velasco, P.C.; Deru, M. Design and dispatch optimization of packaged ice storage systems within a connected community. *Appl. Energy* **2021**, *298*, 117147. [[CrossRef](#)]
39. Song, X.; Liu, L.; Zhu, T.; Chen, S.; Cao, Z. Study of economic feasibility of a compound cool thermal storage system combining chilled water storage and ice storage. *Appl. Therm. Eng.* **2018**, *133*, 613–621. [[CrossRef](#)]
40. Luo, N.; Hong, T.; Li, H.; Jia, R.; Weng, W. Data analytics and optimization of an ice-based energy storage system for commercial buildings. *Appl. Energy* **2017**, *204*, 459–475. [[CrossRef](#)]
41. Beghi, A.; Cecchinato, L.; Rampazzo, M.; Simmini, F. Energy efficient control of HVAC systems with ice cold thermal energy storage. *J. Process Control* **2014**, *24*, 773–781. [[CrossRef](#)]
42. The MathWorks, MATLAB Software: Natick, MA, USA.
43. Sadat-Mohammadi, M.; Asadi, S.; Habibnezhad, M.; Jebelli, H. Robust scheduling of multi-chiller system with chilled-water storage under hourly electricity pricing. *Energy Build.* **2020**, *218*, 110058. [[CrossRef](#)]
44. Huxley, O.T.; Taylor, J.; Everard, A.; Briggs, J.; Tilley, K.; Harwood, J.; Buckley, A. The uncertainties involved in measuring national solar photovoltaic electricity generation. *Renew. Sustain. Energy Rev.* **2022**, *156*, 112000. [[CrossRef](#)]
45. Polemis, M.L. Capturing the impact of shocks on the electricity sector performance in the OECD. *Energy Econ.* **2017**, *66*, 99–107. [[CrossRef](#)]
46. Deng, Z.; Chen, Y.; Yang, J.; Causone, F. AutoBPS: A tool for urban building energy modeling to support energy efficiency improvement at city-scale. *Energy Build.* **2023**, *282*, 112794. [[CrossRef](#)]
47. Chen, Y.; Wei, W.; Song, C.; Ren, Z.; Deng, Z. Rapid Building Energy Modeling Using Prototype Model and Automatic Model Calibration for Retrofit Analysis with Uncertainty. *Buildings* **2023**, *13*, 1427. [[CrossRef](#)]
48. Chen, Y.; Deng, Z.; Hong, T. Automatic and rapid calibration of urban building energy models by learning from energy performance database. *Appl. Energy* **2020**, *277*, 115584. [[CrossRef](#)]
49. GB50189-2005; Energy Efficiency Design Standards for Public Buildings. MOHURD: Beijing, China, 2005.
50. GB50189-2015; Energy Efficiency Design Standards for Public Buildings. MOHURD: Beijing, China, 2015.
51. GB50352-2019; Unified Standard for Design of Civil Buildings. MOHURD: Beijing, China, 2019.
52. GB51161-2016; Standard for Energy Consumption of Building. MOHURD: Beijing, China, 2016.

Disclaimer/Publisher’s Note: The statements, opinions and data contained in all publications are solely those of the individual author(s) and contributor(s) and not of MDPI and/or the editor(s). MDPI and/or the editor(s) disclaim responsibility for any injury to people or property resulting from any ideas, methods, instructions or products referred to in the content.